Limits on the efficiency of several electric thruster configurations[a)]

Amnon Fruchtman[b)]
Holon Academic Institute of Technology, P.O. Box 305, Holon 58102, Israel

(Received 8 November 2002; accepted 21 January 2003)

Limits on the efficiency of several thruster configurations are discussed. The efficiency of the Pulsed Plasma Thruster is reduced when part of the magnetic field energy that is converted into particle energy does not become directed kinetic energy but rather thermal energy. The partitioning of the power when the propellant exhibits slug, snowplow or specular-reflection acceleration is analyzed. It is suggested how to distribute the propellant mass along the accelerating channel so as to efficiently use this thermal energy. Steady acceleration to supersonic velocities is examined in two configurations: the Magneto-Plasma Dynamics (MPD) thruster and the Hall thruster. Limits on the efficiency of the MPD thruster in a nondiverging geometry are derived. The efficiency in the self-field acceleration is higher than in the azimuthal applied-field acceleration. These limits can be overcome in a converging–diverging geometry, analogous to the Laval nozzle, in which the efficiency can approach unity. The acceleration efficiency in the Hall thruster becomes unity for an infinite magnetic Reynolds number even in a nondiverging geometry. The efficiency can be enhanced by the pressure that results from electron heating or by employing segmented emitting electrodes. © *2003 American Institute of Physics.* [DOI: 10.1063/1.1560922]

I. INTRODUCTION

Electric propulsion has the advantage of reduction of the propellant mass needed for a given space mission due to the higher exhaust velocities relative to those achieved by chemical propulsion. Since its introduction in flight in the 1960s, electric propulsion has been advanced and matured, as reviewed in Refs. 1–4. Electric thrusters vary in terms of power (1 W to several MW), exhaust velocities (3 km/s–60 km/s) and type of propellant, according to the mechanism of operation. From among the critical issues for satisfactory operation, efficient ionization, long lifetime, stability, limited plume divergence, proper integration into the spacecraft, and more, I chose to re-examine here one important aspect of electric propulsion, the efficiency of the propellant acceleration. In order to clearly identify the basic limits on the efficiency, I examine the mechanism of acceleration in simplified geometry and adhere to approximated one-dimensional analysis. Electric propulsion thrusters are usually classified as electrothermal, electrostatic and electromagnetic. I discuss here electromagnetic thrusters and analyze three configurations: the Pulsed Plasma Thruster (PPT),[5] the Magneto-Plasma-Dynamics (MPD) thruster,[6] and the Hall thruster.[7]

In the PPT and in the MPD a voltage is applied perpendicular to the direction of acceleration. The work is done by the applied electric field on the electrons that move perpendicular to the direction of acceleration. The energy gained by the electrons is transferred to the accelerated ions. This indirect energy deposition is a possible cause of efficiency reduction. I calculate this efficiency reduction and present an ideal converging–diverging geometry, in which, at the limit of an infinite magnetic Reynolds number, the efficiency becomes unity. The acceleration in the Hall thruster, however, is in the direction of the applied voltage. At the limit of an infinite Reynolds number the efficiency is unity, even in a constant cross-section thruster. Electron heating and segmented electrodes are shown to increase the efficiency in the Hall thruster.

In Sec. II the conversion in the PPT of electromagnetic energy into magnetic field energy that is stored inductively and into particle energy is analyzed. The partitioning of the power in the slug, specular-reflection, and snowplow accelerations is calculated. I then suggest how to specifically distribute the propellant mass along the thruster so as to efffficiently use the thermal energy for ionization. In Sec. III the sonic transition in the MPD and in the Hall thrusters is discussed. In Sec. IV the MPD and the Hall thrusters are compared at the applied field limit. The Hall thruster is shown to be inherently more efficient. In Sec. V the efficiency limit on the self-field MPD of a constant cross section is derived and the enhanced efficiency in an ideal converging-diverging geometry is shown. In Sec. VI it is shown how electron heating and segmented electrodes may enhance the efficiency in the Hall thruster.

II. THE PULSED PLASMA THRUSTER (PPT)

Various complex processes dominate the interaction in the PPT.[8–10] We focus here on intentionally coupling the acceleration and the ionization in order to increase the efficiency. Figure 1 is a schematic of the PPT. A voltage that is applied at the generator drives a current that ionizes the propellant and pushes the generated plasma axially by the associated magnetic field pressure. This pushing of the conducting fluid, by which a part of the electromagnetic field energy is converted into the kinetic energy of the fluid and during which the inductance changes, occurs also in plasma devices

[a)]Paper CI2 5, Bull. Am. Phys. Soc. **47**, 58 (2002).
[b)]Invited speaker.

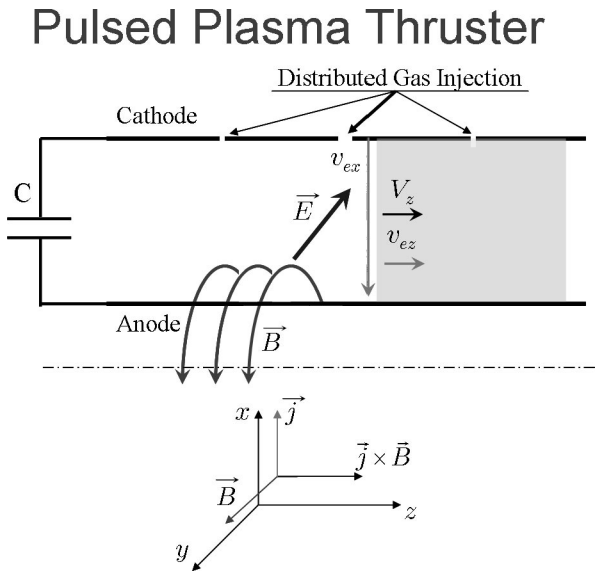

FIG. 1. Schematic of the Pulsed Plasma Thruster: The applied electric field and the current lie in the x direction, perpendicular to the z direction, the direction of acceleration. A narrow current layer separates the unmagnetized plasma from the vacuum permeated by the magnetic field. The ion and electron velocities in the z direction are the same.

such as pinches[11] and plasma opening switches.[12] The power partitioning during the process can be exhibited through employing momentum and energy balance considerations.

Faraday's law and energy balance,

$$E=\frac{d}{dt}(Bz),\quad P_{\mathrm{EM}}=\frac{EB}{\mu_0}=P_B+P_D,$$
$$P_B=\frac{d}{dt}\left(\frac{B^2}{2\mu_0}z\right)\Rightarrow P_D=\frac{B^2\dot{z}}{2\mu_0} \tag{1}$$

govern the dynamics of the system. Here E is the electric field applied between the electrodes in the x direction, B is the magnetic field in the y direction generated by the current, P_{EM} is the Poynting electromagnetic energy flux, P_B and P_D are the rates at which magnetic field energy is stored inductively in the channel and at which electromagnetic energy is dissipated per unit area, respectively, and μ_0 is the permeability of free space. It is assumed that a narrow current layer that is located at a plane z along the acceleration channel separates the unmagnetized propellant from the vacuum region that is permeated by the magnetic field. The dissipated power P_D equals the rate of mechanical work done by the magnetic field pressure. If we write P_D as

$$P_D=\frac{d}{dt}\left(\frac{B^2}{2\mu_0}z\right)-\frac{Bz}{\mu_0}\frac{dB}{dt}, \tag{2}$$

we see that the dissipated power is larger than the rate at which magnetic field energy is being stored inductively only during the decrease of the current. The dissipated power is related to the change in the mechanical momentum of the plasma,

$$P_D=\frac{B^2\dot{z}}{2\mu_0}=\frac{\dot{z}}{hd}\frac{d}{dt}(\mathrm{mV}),\quad \dot{m}=\rho\dot{z},\quad \rho=\frac{1}{hd}\frac{dm}{dz}. \tag{3}$$

Here m and V denote the mass and the velocity of the propellant pushed by the magnetic field pressure, and, in the rectangular geometry, h is the distance between the electrodes, d is the width of each electrode in the y direction and ρ is the mass density. Part of the dissipated power becomes directed kinetic energy of the propellant while the rest becomes heat at rates P_{dKE} and P_{heat} per unit area, respectively,

$$P_D=P_{\mathrm{dKE}}+P_{\mathrm{heat}},\quad P_{\mathrm{dKE}}=\frac{1}{hd}\frac{d}{dt}\left(\frac{mV^2}{2}\right). \tag{4}$$

There are two cases in which all the dissipated power becomes directed kinetic energy, $P_{\mathrm{dKE}}=P_D$. One case is when $\dot{m}=0$ and $V=\dot{z}$, which is slug acceleration. A second case is specular reflection in which the individual ions are elastically scattered by the magnetic piston at a velocity that is twice the momentary $\dot{z}$. In contrast, in the case of snowplow acceleration, ions are inelastically scattered and $V=\dot{z}$ and $P_{\mathrm{heat}}\neq 0$. Obviously, it also occurs that the propellant is neither specularly reflected by the magnetic field pressure, nor pushed as a snowplow, but rather it is pushed at an intermediate velocity, possibly by a shock wave that is caused by the magnetic piston. When both B and ρ are constant in time, the power partitioning is

$$\frac{P_B}{P_{\mathrm{EM}}}=\frac{1}{2}\frac{P_{\mathrm{dKE}}}{P_{\mathrm{EM}}}=\frac{1}{2},\quad P_{\mathrm{heat}}=0;\quad V=2\dot{z}=V_{\mathrm{sr}}=\frac{B}{\sqrt{\mu_0\rho}}, \tag{5}$$

in the case of specular reflection, and

$$\frac{P_B}{P_{\mathrm{EM}}}=\frac{1}{2},\quad \frac{P_{\mathrm{dKE}}}{P_{\mathrm{EM}}}=\frac{1}{4},$$
$$\frac{P_{\mathrm{heat}}}{P_{\mathrm{EM}}}=\frac{1}{4};\quad V=\dot{z}=V_{\mathrm{sp}}=\frac{B}{\sqrt{2\mu_0\rho}}, \tag{6}$$

in the case of a snowplow.

The power that ends up as heat is typically a third of the power that flows into the channel.[9] Part of the generated heat is an essential energy loss that is needed for ion production through evaporation (of a solid propellant) and ionization. The other part of the heat, that results in temperature increase and radiation, is a source of inefficiency. However, if the whole generated heat turns out to be exactly the energy required for complete ionization of the propellant, then, in fact, all dissipated energy is efficiently used, either for ionization or for acceleration. Here I show how to adjust the coupling of the propellant and the electrical circuit so that such a desirable situation occurs.

In the following analysis let us assume that the propellant is pushed as a snowplow. As seen in Eq. (6), if the snowplow velocity is constant, half the dissipated energy only is used for plasma acceleration. In order to use the other half of the dissipated energy for ionization, the kinetic energy gained by each ion should equal the energy needed for the ionization that generates that ion,

$$\frac{m_i V^2}{2}=\alpha_i \epsilon_i \Rightarrow V=\sqrt{\alpha_i}V_{\mathrm{CIV}},\quad V_{\mathrm{CIV}}\equiv\sqrt{\frac{2\epsilon_i}{m_i}}. \tag{7}$$

Here $\alpha_i\epsilon_i$ is the average energy required for ionization, ϵ_i being the ionization energy itself while α_i is a numerical factor that relates ϵ_i to the average energy actually required for ionization in a specified plasma.[13,14] The propellant velocity should, therefore, be approximately V_{CIV}, the critical ionization velocity.[15,16] In order to cause a propagation of the current channel with the desired constant velocity, a judicious design of the mass distribution of the propellant along the channel is required. This technical challenge can be met by the use of a gas-fed pulsed plasma thruster (GFPPT), a concept that is currently being intensively explored.[17] In this type of thruster the propellant distribution can be modified by injecting the gas along the channel through valves of a different cross section.

We continue by analyzing the electrical circuit, adding to the previous analysis a discharged capacitor that supplies the applied voltage, and a finite resistance of the propellant. The circuit equation is

$$\frac{Q}{C}+\frac{d}{dt}[(L_0+L'z)\dot{Q}]+R\dot{Q}=0, \tag{8}$$

where L_0 is the initial inductance, $L'=\mu_0 h/d$ is the inductance per unit length, and $z=0$ denotes the initial location of the plasma boundary at the generator side. The voltage is applied by discharging a capacitor of a capacitance C charged with an electrical charge Q. At the plasma edge, where the plasma is not being pushed yet, the voltage between the electrodes is $R\dot{Q}\simeq(h/da)(\dot{Q}/\sigma)$, where R is the plasma resistance, σ is the plasma conductivity and a is the depth of resistive magnetic field penetration into the plasma. In fact, the resistance can also be written as $R\simeq L'V_d$, where $V_d\equiv 1/(\mu_0\sigma a)$ is the velocity of magnetic field diffusion into the plasma. By multiplying Eq. (8) by $\dot{Q}$ we obtain the conservation of energy,

$$\frac{d}{dt}\left[\frac{Q^2}{2C}+\frac{(L_0+L'z)\dot{Q}^2}{2}\right]+\left(\frac{L'\dot{z}}{2}+R\right)\dot{Q}^2=0. \tag{9}$$

The second term in the equation, the rate of dissipation of electromagnetic field energy, can be written as $P_{\mathrm{diss}}=P_D hd=L'(\dot{z}/2+V_d)\dot{Q}^2$, and expresses the contributions of the dynamic and resistive impedances of the plasma to the dissipation. It is desirable that the dynamic impedance be larger. In terms of the circuit quantities, the momentum equation, that is equivalent to Eq. (3), is

$$\frac{d}{dt}(mV)=\frac{L'\dot{Q}^2}{2}. \tag{10}$$

Since we take the velocity of propagation to be constant $\dot{z}=V$, the inductance becomes simply $L=L_0+L'Vt$. The solution of the equation

$$(L_0+L'Vt)\ddot{Q}+(L'V+R)\dot{Q}+\frac{Q}{C}=0, \tag{11}$$

in which we assume that R and C are constant, and for which the initial current is zero, is

$$Q=\frac{\pi}{2}pQ_0(\sqrt{1+\tau})^{-r}[J_{r+1}(p)Y_r(p\sqrt{1+\tau}) - Y_{r+1}(p)J_r(p\sqrt{1+\tau})], \tag{12}$$

written in terms of Bessel functions. Here,

$$\tau\equiv\frac{L'Vt}{L_0},\quad r\equiv\frac{R}{L'V},\quad p\equiv\frac{2}{L'V}\sqrt{\frac{L_0}{C}}. \tag{13}$$

As an example, we take the limit at which the resistance and the initial inductance are zero, $p=0$ and $r=0$. The charge in the capacitor Q and the current I become

$$Q=Q_0J_0\left(\sqrt{\frac{4t}{L'VC}}\right),\quad I=\frac{Q_0}{\sqrt{L'VCt}}J_1\left(\sqrt{\frac{4t}{L'VC}}\right). \tag{14}$$

The fraction of electromagnetic energy that is converted into particle energy at time t is

$$\frac{U_D}{U_0}=\int_0^s\frac{ds'}{s'}J_1^2(\sqrt{s'})=1-[J_0^2(\sqrt{s})+J_1^2(\sqrt{s})];\quad s\equiv\frac{4t}{L'VC}, \tag{15}$$

where U_D is the energy converted to particle energy and $U_0\equiv Q_0^2/2C$ is the energy initially stored in the capacitor. Although the waveform we treat here is oscillatory and not damped, as is desired for an optimal operation of the PPT,[17] when the voltage reverses and the current is zero most of the magnetic field energy is already drained. Indeed, we can choose the length of the channel, so that the current layer reaches the exit at the time that the current is zero. This value is determined by the first zero of J_1. The acceleration time, the channel length, and the fraction of electromagnetic energy converted into particle energy [calculated using Eq. (15)] are

$$t_d=\frac{3.8317^2}{4}L'VC;\quad l_d=Vt_d;\quad \frac{U_D}{U_0}=1-J_0^2(3.8317)=0.837\,78,\quad \frac{U_{\mathrm{dKE}}}{U_0}=0.418\,89. \tag{16}$$

Here U_{dKE} is the electromagnetic energy converted into directed kinetic energy of the propellant. The same amount of energy is used for ionization. The appropriate distribution of the propellant mass is derived from the momentum equation, Eq. (10). The density is adjusted according to the current, so that the snowplow velocity is constant. The density distribution turns out to be

$$\frac{dm}{dz}=\frac{L'I^2}{2V^2}=\frac{Q_0^2}{2CV^3t}J_1^2\left(\sqrt{\frac{4t}{L'VC}}\right). \tag{17}$$

Figure 2 presents the normalized applied voltage $Q_N\equiv Q/Q_0$, current $I_N\equiv IL'VC/Q_0$, and mass distribution $m'_N\equiv(dm/dz)(C^2V^4L'/Q_0^2)$ as a function of the normalized location of the current layer along the channel z/Vt_d. More

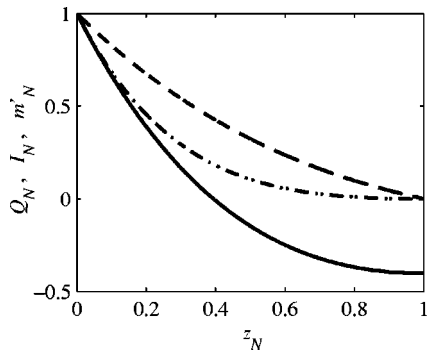

FIG. 2. The Pulsed Plasma Thruster: The normalized applied voltage $Q_N \equiv Q/Q_0$ (solid), current $I_N \equiv IL'VC/Q_0$ (dashed), and mass distribution $m'_N \equiv (dm/dz)(C^2V^4L'/Q_0^2)$ (dotted–dashed) vs the normalized location of the current layer along the channel z/Vt_d.

realistic distributions could be designed for finite values of R and L_0. A finite L_0 results in $I_N=0=m'_N$ at $z=0$.

It is desirable to have exhaust velocities higher than V_{CIV}. The idea sketched above should then be implemented in the ionization section only. An acceleration of the ionized plasma to a higher velocity as a slug that follows the snow-plow pushing results in a higher efficiency.

III. THE SONIC TRANSITION IN STEADY ACCELERATORS

Let us turn now to steady electromagnetic accelerators. The two configurations we will address are the MPD and the Hall thruster, shown schematically in Figs. 3 and 4.

The governing equations for the two thrusters are the standard fluid equations, which we write for a one-dimensional geometry. These are the continuity equation

$$\frac{\partial(nV_z)}{\partial z}=S, \tag{18}$$

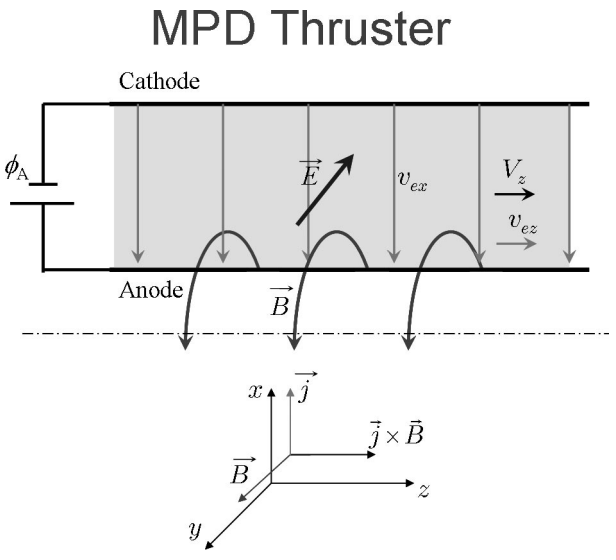

FIG. 3. Schematic of the MPD thruster: The applied electric field and the current lie in the x direction, perpendicular to the z direction, the direction of acceleration. The ion and electron velocities in the z direction are the same. The current is distributed along the channel.

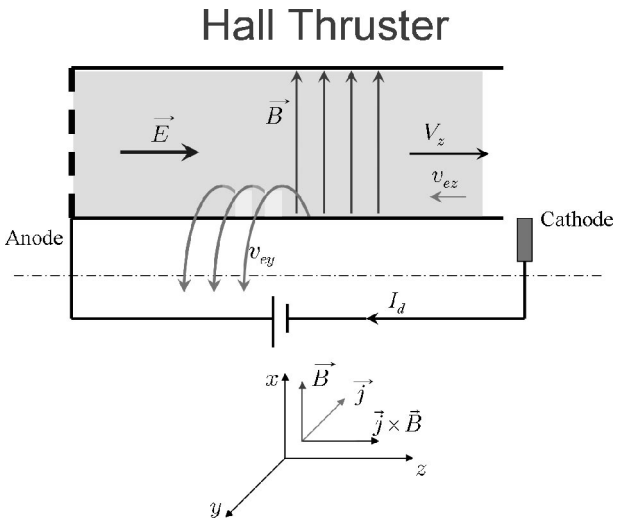

FIG. 4. Schematic of the Hall thruster: The electric field is applied in the z direction, the direction of acceleration. The ion and electron velocities in the z direction are different.

the momentum equation,

$$m_iV_z\frac{dV_{x,z}}{dz}=e(E_{x,z}\mp V_{z,x}B)-\nu m_e(V_{x,z}-v_{x,z}) - \frac{m_iSV_{x,z}}{n}, \tag{19}$$

the electron momentum equation,

$$0=-e(E_{x,z}\mp v_{z,x}B)-\nu m_e(v_{x,z}-V_{x,z})-\frac{1}{n}\hat{e}_z\cdot\nabla P \tag{20}$$

(the minus and plus signs refer to the x and to the z components, respectively), and the energy equation,

$$\frac{d}{dz}\left(\frac{5}{2}nv_eT\right)=-en\mathbf{E}\cdot\mathbf{v}-S\alpha_i\epsilon_i. \tag{21}$$

As usual, $V_{z,x}$ and $v_{z,x}$ are the components of the ion and electron velocities, n, T, and P are the electron density, temperature, and pressure, the enthalpy is $(5/2)T$, S is the source term, and $\mathbf{E}\cdot\mathbf{v}=-(\nu m_e/e)[v_x^2+v_z(v_z-V_z)]-(v_z/en)\times(\partial P/\partial z)$. The ion temperature is neglected. Assuming $v_x^2 \gg v_z(v_z-V_z)$, we find that

$$(V_z^2-V_s^2)\frac{dV_z}{dz}=-\frac{ev_xBV_z}{m_i}-\frac{2}{3}\frac{\nu m_eV_zv_x^2}{m_iv_z} + \frac{S}{n}\left[\frac{V_z[(5/2)T+\alpha_i\epsilon_i]}{m_iv_z}-(V_z^2+V_s^2)\right]. \tag{22}$$

Here the sonic velocity is $V_s^2\equiv(5/3)(T/m_i)$. A similar version of this equation that allows also a varying cross section is included in a comprehensive analysis of the MPD interaction.[6] The equation here (22), in which the ion and electron velocities in the z direction (the direction of acceleration) are not necessarily the same, holds for both constant cross section MPD and Hall thrusters.

Let us examine the transition to supersonic velocities in both thrusters. In order for a smooth transition to supersonic velocities to occur the right-hand side (RHS) of Eq. (22) has to vanish at the sonic velocity. The first term on the right-hand side (RHS) of Eq. (22) expresses the magnetic field force and is always positive. The second term represents the effect of heating on the acceleration. It turns out that heating contributes to the acceleration in the Hall thruster, while it serves as a drag in the MPD. Formally this is a result of the fact that this second term in the equation is positive in the Hall thruster (in which ions and electrons move in opposite directions, $V_z>0$ and $v_z<0$) and negative in the MPD (in which $V_z=v_z$). The reason for these opposite roles is that in the Hall thruster electrons heat up while they move into the thruster away from the exit, in contrast to the MPD thruster in which electrons heat up while they move towards the exit. The temperature increase contributes to the accelerating role of the pressure gradient in the Hall thruster while it weakens this role in the MPD thruster. Because the heating results in a drag force in the MPD, the RHS of Eq. (22) may vanish at the sonic velocity. Smooth sonic transition can occur in the MPD thruster even if $S=0$, as it is in the acceleration channel beyond the ionization region. In the Hall thruster however, in which the heating term is positive, a smooth sonic transition can occur only where ionization [the third term in Eq. (22)] is not zero.[18,19]

IV. APPLIED-FIELD STEADY THRUSTERS

The efficiency of the thruster is defined as

$$\eta=\frac{F^2}{2\dot{m}\int_0^l \mathbf{j}\cdot\mathbf{E}dz}=\frac{(1/2)V_{zf}\int_0^l j_x B dz}{\int_0^l \mathbf{j}\cdot\mathbf{E}dz}, \tag{23}$$

where the thrust is $F\equiv\dot{m}V_{zf}=m_i h d n_f V_{zf}^2$. Quantities that are denoted by the subscript f mean their value at the exit of the thruster. Employing the notations in Figs. 3 and 4, we note that in the MPD thruster the energy is first deposited in the electrons (through $j_x E_x$), energy that the electrons lose in their axial motion to the ions that are accelerated by the axial electric field. In the Hall thruster however, the energy is deposited directly in the accelerated ions (through $j_z E_z$). We will first discuss this efficiency in the cold plasma limit, assuming that T is small. Later, we will address the finite temperature Hall thruster, recognizing the possible contribution of the electron heating to the acceleration in the Hall thruster, discussed in the previous section.

In this section we will examine the efficiency of thrusters in which the self-magnetic field due to the current is much smaller than the applied magnetic field. This is the usual situation in the Hall thruster in which self-fields are much smaller than the radial (in the x direction) applied magnetic field. In the MPD thruster, in addition to the self-magnetic field that is azimuthal (in the y direction), a radial magnetic field is sometimes applied.[4] In our analysis of the MPD thruster however, we assume that both applied and self magnetic fields are azimuthal. Also, for simplicity, we assume that this applied magnetic field is uniform.

Let us first discuss the MPD, as is schematically shown in Fig. 3. In the MPD of a uniform cross section the electric field is uniform and points in the x direction. Therefore,

$$\eta_{\mathrm{MPD}}=\frac{(1/2)V_{zf}\int_0^l j_x B dz}{E_x\int_0^l j_x dz}\leqslant\frac{(1/2)V_{zf}\int_0^l j_x B dz}{V_z B\int_0^l j_x dz}, \tag{24}$$

since $E_x\geqslant V_z B$. In the case of a strong uniform applied magnetic field (in the y direction, the same direction as that of the self-field) $B=B_0$, the maximal efficiency becomes half,

$$\eta_{\mathrm{MPD}}^l\leqslant 0.5. \tag{25}$$

Using the linearized z component of the momentum equation and the x component of the electron momentum equation, with the relation $\phi_A=E_x h$, we obtain explicitly that

$$D=1-b-\frac{1}{R_M}\frac{db}{d\xi};\quad b\equiv\frac{B}{B_0},\quad \xi\equiv\frac{z}{l}, \tag{26}$$

with the parameters

$$D\equiv\frac{\phi_A}{2hV_{z,\max}B_0},\quad \frac{1}{R_M}\equiv\frac{v_d}{2V_{z,\max}},$$
$$v_d\equiv\frac{\nu m_e}{\mu_0 e^2 n l},\quad V_{z,\max}\equiv\frac{hB_0^2}{2\mu_0 m_i\Gamma},\quad \Gamma\equiv nV_z h. \tag{27}$$

Here $V_{z,\max}$ is not the actual maximal velocity, but rather the maximal velocity obtained in the nonlinear regime by magnetic field pressure, v_d is the diffusion velocity of the magnetic field into a plasma of length l, which is the length of the acceleration channel. I assume that the collision frequency is proportional to the plasma density, as it is in binary collisions. Solving Eq. (26) and the ion momentum equation, we find that the magnetic field and the ion velocity along the channel are

$$B=B_0\{1-D[1-\exp(-R_M\xi)]\},\quad V_z=\frac{hB_0(B_0-B)}{m_i\Gamma\mu_0}, \tag{28}$$

and therefore the efficiency is

$$\eta_{\mathrm{MPD}}^l=\tfrac{1}{2}[1-\exp(-R_M)]. \tag{29}$$

In the Hall thruster an electric field is applied in the direction of acceleration. In a uniform magnetic field and a cold plasma the efficiency becomes

$$\eta_{\mathrm{Hall}}=\frac{m_i n_f V_{zf}^3/2}{\int_0^l \mathbf{j}\cdot\mathbf{E}dz}=\frac{1}{1+|v_{ez}|/V_z}=\frac{1}{1+1/R_M}. \tag{30}$$

In contrast to the MPD, for the Hall thruster I assume that the collisionality of the electrons is anomalous[14] and therefore its frequency is independent of the plasma density.

The Hall thruster does not have the 0.5 barrier for the efficiency and is therefore inherently more efficient than the MPD thruster. In reality, however, the efficiency of Hall thrusters has never exceeded 55%. Some efficiency reduction is unavoidable since energy must also be used for ionization.[20] Moreover, interaction with the walls,[21] oscillations,[22] and plume divergence[23–26] further reduce the efficiency. The unavoidable efficiency reduction due to the use of part of the power for ionization equals the ratio of the

ionization energy to the maximal ion kinetic energy, and, for both the MPD and the Hall thruster, it turns out to be only a few percent.

V. MPD ENHANCED EFFICIENCY

Here we show how the efficiency in the MPD is increased to above 0.5 by operating with self-fields and by geometry. Let us first analyze the self-field MPD. Employing Eqs. (19) and (20) at the limit of cold electrons ($P=0$), we derive the relation between the flow velocity and the intensity of the magnetic field along the channel,

$$m_i \frac{\Gamma}{h} V_z = \frac{B_0^2 - B^2}{2\mu_0}. \tag{31}$$

Performing the integrals in Eq. (24) we obtain

$$\eta = \frac{h^2}{8 m_i \Gamma} \frac{B_0^3}{\phi_A \mu_0} = \frac{1}{8D}. \tag{32}$$

The maximal efficiency is reached when ϕ_A and D obtain their minimal values. From the nonlinear version of Eq. (26),

$$D = \frac{(1-b^2)b}{2} - \frac{1}{R_M} \frac{\partial b}{\partial \xi}, \tag{33}$$

the minimal values of ϕ_A and of D are reached for $\nu=0$ when $(1-b^2)b$ is maximal, which, in turn occurs for $b=1/\sqrt{3}$. The minimal value of D, substituted in Eq. (32), yields a maximal value for the efficiency,

$$\eta_{\mathrm{MPD}}^{nl} \leqslant \frac{3\sqrt{3}}{8} = 0.649\,52. \tag{34}$$

This value is higher than in the applied field case (25) but still smaller than unity. This efficiency limit and also explicit profiles of the magnetic field are given in Refs. 27 and 6.

The limit on the efficiency can be relaxed if the cross section of the channel is not uniform. Indeed, an incease in efficiency by geometry has been shown[27,6] and analyzed in a two-dimensional model.[28] Here, within a quasi-one-dimensional model, an acceleration of a plasma in the MPD configuration is presented, that relies on a converging-diverging geometry, similar to the acceleration of a gas through a Laval nozzle. The theoretical limit on the efficiency in this case is unity.

The combination of the continuity equation and momentum equation under a pressure gradient,

$$n m_i V_z \frac{dV_z}{dz} = -\frac{dP}{dz}, \tag{35}$$

yields, when the pressure P depends on the plasma mass density ρ only,

$$\left(V_z^2 - \frac{\partial P}{\partial \rho} \right) \frac{dV_z}{dz} = V_z \frac{\partial P}{\partial \rho} \frac{d \ln h}{dz}. \tag{36}$$

In a magnetized cold plasma the pressure in the momentum equation is the magnetic field pressure $P_B \equiv B^2/2\mu_0$. In a collisionless plasma (an infinite R_M) the magnetic field intensity is linearly proportional to the plasma density (the magnetic field is frozen into the electron fluid),

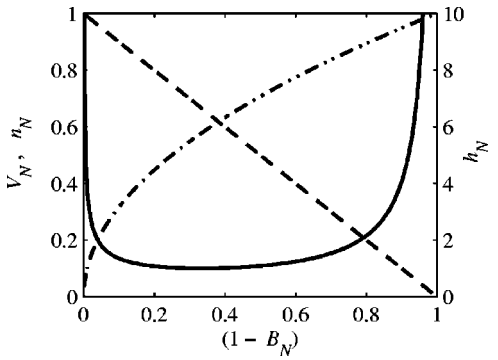

FIG. 5. The normalized velocity $V_{z,N} \equiv V_z/V_{z,\max}$ (dotted–dashed), density $n_N \equiv n\phi_A/(\Gamma B_0)$ (dashed), and distance between the electrodes $h_N \equiv h/h_{\mathrm{neck}}$ (solid) vs $1-B_N$, ($B_N \equiv B/B_0$) in a converging–diverging MPD.

$$\frac{\phi_A}{h} = E_x = V_z B \Rightarrow \frac{B}{n} = \frac{\phi_A}{\Gamma} \Rightarrow P_B = \frac{n^2 \phi_A^2}{2\mu_0 \Gamma^2}$$

$$\Rightarrow \frac{\partial P_B}{\partial \rho} = V_{MS}^2 \equiv \frac{B^2}{\mu_0 m_i n}, \tag{37}$$

and Eq. (36) becomes

$$(V_z^2 - V_{MS}^2) \frac{dV_z}{dz} = V_z V_{MS}^2 \frac{d \ln h}{dz}. \tag{38}$$

The velocity V_{MS} is a characteristic velocity of a magnetized flow, as described in Ref. 29.

Integrating the equations directly we obtain V_z, h, and n as a function of B,

$$V_z^2 = \frac{2\phi_A}{m_i \Gamma \mu_0}(B_0 - B), \quad h^2 = \frac{\phi_A \Gamma \mu_0 m_i}{2B^2(B_0 - B)}, \quad n = \frac{\Gamma B}{\phi_A}. \tag{39}$$

In the converging part of the channel $V_z < V_{MS}$ while in the diverging part $V_z > V_{MS}$. The flow velocity increases from zero to a finite value and the density decreases from a finite value to zero, while the distance between the electrodes is infinite at both ends and reaches a minimal value at the channel neck, where $dh^2/dB = 0$. At the neck

$$B_{\mathrm{neck}} = \tfrac{2}{3} B_0; \quad V_{z,\mathrm{neck}}^2 = V_{MS}^2 = \frac{2\phi_A B_0}{3\mu_0 m_i \Gamma} = \frac{V_{z,\max}^2}{3};$$

$$h_{\mathrm{neck}}^2 = \frac{27 \phi_A \mu_0 m_i \Gamma}{8 B_0^3}; \quad n_{\mathrm{neck}} = \frac{2\Gamma B_0}{3\phi_A}. \tag{40}$$

Figure 5 shows $V_{z,N} \equiv V_z/V_{z,\max}$, $n_N \equiv n\phi_A/(\Gamma B_0)$, and $h_N \equiv h/h_{\mathrm{neck}}$ as a function of $1 - B/B_0$. The efficiency is unity,

$$\eta = \frac{F^2}{2\dot{m}\phi_A I} = \frac{\Gamma m_i V_{zf}^2/2}{\phi_A B_0/\mu_0} = 1. \tag{41}$$

By specifying $\dot{m} = m_i \Gamma d$, ϕ_A, and h_{neck}, the current $I = dB_0/\mu_0$ is specified

$$I^3=\frac{27\phi_A\dot{m}d^2}{8\mu_0^2h_{\rm neck}^2}. \tag{42}$$

For completeness we also write the thrust in the converging-diverging MPD,

$$F=\dot{m}V_{zf}=\frac{4\mu_0}{3\sqrt{3}}\frac{h_{\rm neck}}{d}I^2. \tag{43}$$

In the next section we discuss ways by which to enhance the efficiency in the Hall thruster.

VI. HALL THRUSTER ENHANCED EFFICIENCY

As we saw in Sec. IV, the efficiency in the Hall thruster approaches unity, theoretically, as R_M is increased. It has been shown that if there are no losses, the electron temperature should reach a value of $0.3e\phi_A$ at the sonic transition plane.[14] It has been demonstrated[20] by use of momentum and energy balance, that for a given R_M, the efficiency of the Hall thruster is significantly enhanced by this electron heating. The dependence of the efficiency on R_M is no longer described by Eq. (30) but rather by

$$\eta_{\rm Hall}=\frac{1}{1+1/(5R_M)}. \tag{44}$$

However, theoretical calculations of the Hall thruster that include wall losses, such as those described in Refs. 30–32, showed much lower temperatures than those expected with no wall losses.[14] Thus, one major source of inefficiency in the Hall thruster that results from the cooling of the electrons by collisions with the wall is the loss of particle pressure that could otherwise contribute to the acceleration.

Minimizing the energy deposited in the electrons through the introduction of segmented electrodes into the Hall thruster has been explored recently both experimentally[33] and theoretically.[19,34] Here, we examine this idea by the variational method that was introduced in Ref. 34. In the acceleration region the density of the ions that fall down the electrostatic potential equals the density of the electrons that move across the magnetic field due to their collisionality,

$$\frac{\Gamma_i}{(1-\psi)^{1/2}}=\frac{\Gamma_e}{f(\psi)d\psi/d\zeta};\quad \psi\equiv\frac{\phi}{\phi_A};$$
$$\frac{d}{d\zeta}\equiv\left(\frac{e}{2m\phi_A}\right)^{1/2}\frac{\overline{\nu}(z)\phi_A}{\omega_c^2}\frac{d}{dz}. \tag{45}$$

The collision frequency ν is assumed of the form $\nu=\overline{\nu}(z)f(\psi)$ and $f(0)=1$. In the presence of segmented electrodes the electron flux Γ_e is not constant along the channel. The efficiency is

$$\eta=\frac{1}{1+\int_0^{\zeta_T}d\zeta F(\psi,\psi')};\quad F(\psi,\psi')\equiv\frac{f(\psi)(\psi')^2}{(1-\psi)^{1/2}};$$
$$\psi'\equiv\frac{d\psi}{d\zeta};\quad \zeta_T\equiv\zeta(z=L). \tag{46}$$

For specified magnetic field $\omega_c^2(z)$ and collision $\overline{\nu}(z)$ profiles, so that $\zeta(z)$ and ζ_T are specified, we look for the optimal $\psi(\zeta)$ and the associated optimal $\Gamma_e(\zeta)$. Interestingly, for F of the form in Eq. (46), $\psi(\zeta)$ that satisfies Euler's equation, $(\partial/\partial\zeta)(\partial F/\partial\psi')-\partial F/\partial\psi=0$, also satisfies $dF/d\zeta=0$. Therefore, the work done on the electrons is minimal when it is uniform along the acceleration channel [$F(\zeta)$ is constant].

The case $f(\psi)=1$ was examined in Ref. 34 and the optimal distribution of the electric potential resulted in only a small efficiency enhancement with respect to the regular one-cathode configuration. Here a case is examined in which the collision frequency (due, possibly, to an instability-related anomalous collisionality) varies linearly with the plasma frequency, $f(\psi)=(1-\psi)^{-1/4}$. For the regular flow, in which Γ_e is constant,

$$\psi_r=1-\left(\frac{\zeta}{\zeta_T}\right)^4;\quad \Gamma_{e,r}=-\frac{4}{\zeta_T};\quad \eta_r=\frac{1}{1+4/\zeta_T}. \tag{47}$$

The optimal flow, for which $dF/d\zeta=0$, turns out to be

$$\psi_{\rm opt}=1-\left(\frac{\zeta}{\zeta_T}\right)^{8/5};\quad \Gamma_{e,{\rm opt}}=-\frac{8}{5\zeta_T}\left(\frac{\zeta_T}{\zeta}\right)^{3/5};$$
$$\eta_{\rm opt}=\frac{1}{1+64/(25\zeta_T)};\quad \lim_{\zeta_T\to 0}\frac{\eta_{\rm opt}}{\eta_r}=1.56. \tag{48}$$

As a more practical example than the continuous distribution of current emission, let us assume that we apply a potential $\psi=\psi_1$ at a single electrode that we insert at a position $\zeta=\zeta_1$ between the cathode and the anode. As in Ref. 34, the constant electron flow in the region $\zeta_1>\zeta>0$ is denoted by Γ_1 and the constant electron flow in the region $\zeta_T>\zeta>\zeta_1$ by Γ_2 (the flow from the cathode). Integrating Eq. (45) in the two regions, we obtain the relations $-\Gamma_1\zeta_1=4(1-\psi_1)^{1/4}$ and $-\Gamma_2(\zeta_T-\zeta_1)=4-4(1-\psi_1)^{1/4}$. The efficiency is expressed as $\eta_1=[1-\Gamma_1(\psi_i-\psi_1)-\Gamma_2\psi_1]^{-1}$. We find the maximal efficiency by solving $\partial\eta_1/\partial\zeta_1=0$ and $\partial\eta_1/\partial\psi_1=0$ to find $\zeta_1/\zeta_T=0.19121$ and $\psi_1=0.94419$. Then,

$$\eta_{1,{\rm opt}}=\frac{1}{1+4\times 0.74186/\zeta_T};\quad \lim_{\zeta_T\to 0}\frac{\eta_{1,{\rm opt}}}{\eta_r}=1.35. \tag{49}$$

For low magnetic field intensity the efficiecy enhancement is significant.

VII. CONCLUSIONS

Limits on the efficiency of three electromagnetic thruster configurations have been derived and compared. Ways to increase the efficiency of these devices have been discussed. For the PPT it is proposed how to distribute the propellant mass along the accelerating channel so as to efficiently use the thermal energy that results from the dissipation of the electromagnetic energy. The important role of geometry and the advantage of a converging–diverging geometry in the MPD configuration have been demonstrated. The Hall thruster has been shown to be inherently more efficient than the MPD. The analysis here, however, has been performed

using certain simplifying assumptions. Many complex processes not taken into account here make the physical picture less clear. I hope that the ideas presented here will help in performing a more detailed analysis of the operation of electric thrusters.

ACKNOWLEDGMENTS

The author is grateful to A. Cohen-Zur, G. Makrinich, Professor N. J. Fisch, Dr. Y. Raitses, and Professor E. Y. Choueiri for helpful discussions.

This research has been partially supported by a Grant No. 9800145 from the United States–Israel Binational Science Foundation (BSF), Jerusalem, Israel, and by a Grant No. 59/99 from the Israel Science Foundation.

[1]R. G. Jahn, *Physics of Electric Propulsion* (McGraw-Hill, New York, 1968).
[2]P. J. Wilbur, R. G. Jahn, and F. C. Curran, IEEE Trans. Plasma Sci. **19**, 1167 (1991).
[3]R. M. Myers, AIAA Paper No. 93-1086, *Aerospace Design Conference*, Irvine, CA (American Institute of Aeronautics and Astronautics, Washington, D.C., 1993).
[4]M. Martinez-Sanchez and J. E. Pollard, J. Propul. Power **14**, 688 (1998).
[5]R. L. Burton and P. J. Turchi, J. Propul. Power **14**, 716 (1998).
[6]M. Martinez-Sanchez, J. Propul. Power **7**, 56 (1991).
[7]A. I. Morozov, Yu. V. Esipchuk, G. N. Tilinin, A. V. Trofinov, Yu. A. Sharov, and G. Ya. Shahepkin, Sov. Phys. Tech. Phys. **17**, 38 (1972).
[8]P. J. Turchi, R. J. Leiweke, and H. Kamhawi, AIAA Paper No. 96-2731, *32th Joint Propulsion Conference*, Lake Buena Vista, FL (American Institute of Aeronautics and Astronautics, Washington, D.C., 1996).
[9]R. L. Burton, M. J. Wilson, and S. S. Bushman, AIAA Paper No. 98-3808, *34th Joint Propulsion Conference*, Cleveland, OH (American Institute of Aeronautics and Astronautics, Washington, D.C., 1998).
[10]G. G. Spanjers, J. S. Lotspeich, K. A. McFall, and R. A. Spores, J. Propul. Power **14**, 554 (1998).
[11]M. A. Liberman, J. S. De Groot, A. Toor, and R. B. Spielman, *High-Density Z-Pinch Plasmas* (Springer, New York, 1998).
[12]C. W. Mendel, Jr. and S. A. Goldstein, J. Appl. Phys. **48**, 1004 (1977); G. Cooperstein and P. F. Ottinger, IEEE Trans. Plasma Sci. **PS-15**, 629 (1987).
[13]M. A. Lieberman and A. J. Lichtenberg, *Principles of Plasma Discharges and Materials Processing* (Wiley, New York, 1994).
[14]E. Ahedo, P. Martinez-Cerezo, and M. Martinez-Sanchez, Phys. Plasmas **8**, 3058 (2001).
[15]J. A. Marshall, J. L. Burch, E. Y. Choueiri, and N. Kawashima, Geophys. Res. Lett. **20**, 499 (1993).
[16]N. Brenning, Space Sci. Rev. **59**, 209 (1992).
[17]J. K. Ziemer and E. Y. Choueiri, Plasma Sources Sci. Technol. **10**, 395 (2001).
[18]A. Fruchtman, N.J. Fisch, J. Ashkenazy, and Y. Raitses, IEPC Paper No. 97-022, *25th International Electric Propulsion Conference*, Cleveland, OH (Electric Rocket Propulsion Society, Cleveland, OH, 1997).
[19]A. Fruchtman, N. J. Fisch, and Y. Raitses, Phys. Plasmas **8**, 1048 (2001).
[20]A. Cohen-Zur, A. Fruchtman, J. Ashkenazy, and A. Gany, Phys. Plasmas **9**, 4363 (2002).
[21]Y. Raitses, J. Ashkenazy, G. Appelbaum, and M. Guelman, IEPC Paper No. 97-056, *25th International Electric Propulsion Conference*, Cleveland, OH (Electric Rocket Propulsion Society, Cleveland, OH, 1997).
[22]J. P. Boeuf and L. Garrigues, J. Appl. Phys. **84**, 3541 (1998); N. B. Meezan, W. A. Hargus, Jr., and M. A. Cappelli, Phys. Rev. E **63**, 026410 (2001).
[23]L. B. King and A. D. Gallimore, J. Propul. Power **16**, 916 (2000).
[24]I. Katz, G. Jongeward, V. Davis, M. Mandell, I. Mikellides, R. Dresseler, I. Boyd, K. Kannenberg, J. Pollard, and D. King, AIAA Paper No. 2001-3355, *37th Joint Propulsion Conference* (American Institute of Aeronautics and Astronautics, Washington, D.C., 2001).
[25]M. Andrenucci, L. Biagioni, and A. Passaro, AIAA Paper No. 2002-4254, *38th Joint Propulsion Conference*, Indianapolis, IN (American Institute of Aeronautics and Astronautics, Washington, D.C., 2002).
[26]J. Ashkenazy, Y. Raitses, and G. Appelbaum, Phys. Plasmas **5**, 2055 (1998).
[27]K. Kuriki, Y. Kunii, and Y. Shinizu, AIAA Paper No. 81-0685, 15*th International Electric Propulsion Conference*, Las Vegas, NV (American Institute of Aeronautics and Astronautics, New York, 1981).
[28]A. I. Morozov and L. S. Solov'ev, *Steady-State Plasma Flow in a Magnetic Field*, in *Reviews of Plasma Physics*, edited by M. A. Leontovich (Consultants Bureau, New York, 1980), Vol. 8, p. 1.
[29]E. L. Resler, Jr. and W. R. Sears, J. Aeronaut. Sci. **25**, 235 (1958).
[30]E. Ahedo, P. Martinez-Cerezo, J. M. Gallardo, and M. Martinez-Sanchez, IEPC Paper No. 01-017, *27th International Electric Propulsion Conference*, Pasadena, CA (Electric Rocket Propulsion Society, Cleveland, OH, 2001).
[31]K. Makowski, Z. Peradzynski, N. Gascon, and M. Dudeck, AIAA Paper No. 99-2295, *35th Joint Propulsion Conference*, Los Angeles, CA (American Institute of Aeronautics and Astronautics, Washington, D.C., 1999).
[32]M. Keidar, I. D. Boyd, and I. I. Bellis, Phys. Plasmas **8**, 5315 (2001).
[33]Y. Raitses, L. A. Dorf, A. A. Litvak, and N. J. Fisch, J. Appl. Phys. **88**, 1263 (2000).
[34]A. Fruchtman and N. J. Fisch, Phys. Plasmas **8**, 56 (2001).